3D PRINTING AND ADDITIVE MANUFACTURING
Volume 11, Number 6, 2024

DOI: 10.1089/3dp.2023.0151

ORIGINAL ARTICLE

Effect of Graphene-Based Coating 3D Printing Process on the Remanence and Corrosion of Sintered NdFeB Magnets

Julio Cesar Serafim Casini,[1] Isolda Costa,[2] and Rubens Nunes de Faria Jr.[2]

Abstract

This study describes a 3D fused deposition modeling (FDM) printing process using a graphene-impregnated polylactic acid (G-PLA) filament to create a new type of rigid, plastic, nonconductive, and anticorrosion layer. Therefore, the possibility of 3D printing a plastic layer using FDM methods is demonstrated herein. A commercial magnet such as N35 NdFeB can be used to produce an efficient shielding film by additive manufacturing. As the coating layer thickness increases, the remanence decreases from 1.17 to 1.01 T for the G-PLA coating. Visual tests were performed after exposure to all aqueous NaCl test solutions (0.5 and 1 M), and no evidence of corrosion of the coating was obtained.

Keywords: NdFeB magnets, graphene, 3D printed

Introduction

Owing to the remarkable ability of sintered NdFeB magnets to generate magnetic fields without high electricity or heat generation expenditures, these magnets are widely used in electromechanical devices.[1] However, the low corrosion resistance of these magnets limits their commercial applications. This low resistance can be attributed to the multiphase microstructure of the matrix phase and the presence of intergranular phases, such as Nd- and B-rich phases. It is to be noted that intergranular phases with high electrochemical activity exhibit high corrosion rates.[2]

Researchers have devoted considerable efforts to improving the corrosion resistance of NdFeB magnets. Some researchers have used alloy replacement elements such as cobalt, aluminum, copper, and niobium.[3,4] Others have synthesized new coatings that insulate magnets from corrosive environments.[5,6] Typically, the corrosion behavior of magnets is investigated by exposing them to a neutral saline solution. Several other strategies have been reported for enhancing the corrosion resistance of NdFeB magnets.[7–17] Graphene has also been reported as an effective coating for improving the corrosion resistance of copper, steel, and NdFeB magnets.[18–25]

Additive manufacturing refers to the layer-by-layer process of building apart from the material. This technology allows the fabrication of complex geometries without being constrained by the skills of tools or molds, as in other types of fabrication. Several types of additive manufacturing have been developed by researchers. The most widespread, common, and least expensive technology is fused deposition modeling (FDM). FDM, often referred to as 3D printing, involves heating a material (most commonly a thermoplastic polymer) in a nozzle and continuously extruding the viscous material onto a print bed to create a layer.

When one layer is complete, the printer head raises a fraction of a millimeter so that the subsequent layer can be extruded and deposited. This process is repeated until all layers are extruded.[26] The use of thermoplastic polymers with low melting temperatures and short solidification times has drawn attention owing to their simplicity and low manufacturing costs. For example, polylactic acid (PLA) is in considerable demand worldwide owing to its versatile applicability in packaging, pharmaceuticals, textiles, automotive, biomedical, and tissue engineering. It has been widely investigated for biomedical applications owing to its biodegradability and biocompatibility.[27,28]

Ongoing efforts are consistently being directed toward enhancing the properties of commonly used thermoplastics through the integration of particles, fibers, or nanomaterial reinforcements.[29] Graphene has gained remarkable popularity

[1]Federal Institute of Education, Science and Technology of São Paulo Campus, São José dos Campos–IFSP-SJC, São José dos Campos, São Paulo, Brazil.
[2]Materials Science and Technology Center (CCTM), Nuclear, and Energy Research Institute (IPEN), University of São Paulo (USP), São Paulo, São Paulo, Brazil.

owing to its exceptional attributes, particularly when infused into PLA for 3D printing applications.[30] This filament offers enhanced operational temperature performance, heightened rigidity, substantial impact resistance, and excellent interlayer adhesion, resulting in seamless printing. Extensive research endeavors are being pursued to harness the distinctive attributes of graphene-impregnated polylactic acid (G-PLA) material within the context of the fused filament fabrication process.

Multiple studies have elucidated the positive effects of graphene nanoplatelet reinforcement, showcasing its capacity to augment mechanical properties, dimensional accuracy, and surface texture of PLA components. These illustrative instances underscore the significance of G-PLA material augmented with graphene, underscoring the necessity to comprehend the combined influence of process parameters and the imperative for optimization to attain desired outcomes.[31–33]

The combination of FDM with an appropriate software package allows for a fully customizable printed part geometry. Several parameters can be customized to enhance or make printed parts more flexible. These features include the fill factor (percentage density or concentration of the extruded lines), outer layer thickness (boxes), and fill pattern. The selection of such features can be applied to the properties of the final printed product.

The coatings currently applied to NdFeB magnets are produced using the electroplating technique, which requires an initial pretreatment involving immersion in chemical agents to perform initial etching, followed by the electrochemical deposition of nickel layers through chemical baths. In contrast, the approach of utilizing biodegradable materials such as PLA and G-PLA using the 3D printing technique for the fabrication of corrosion-resistant coatings opens a new perspective for future investigations in this field. In this study, the construction of a 3D printed coating with a thermoplastic polymer–graphene composite material by FDM was explored. First, the successful printing of a coating with the geometry of commercial NdFeB magnets by FDM was demonstrated. Then, the long-term corrosion behaviors of the N35 NdFeB magnet in NaCl test solutions (0.5 and 1 M) were investigated from 0 to 30 days by immersion tests.

Materials and Methods

Coating preparation

The coating was fabricated through a printing process, employing a composite polymeric matrix of PLA with graphene (G-PLA), utilizing filaments with a diameter of 1.75 mm, supplied by 3D Haydale Ltd., headquartered in Loughborough, United Kingdom. The methodology is rooted in the specifications provided in the datasheet issued by Haydale, detailing the integration of functionalized graphene nanoplatelets, featuring planar dimensions ranging from 0.3 to 5 μm. The PLA employed originated from the biopolymer NatureWork 4043D Ingeo.[34] The characteristics of G-PLA are shown in Table 1.

A custom 3D printer, an upgraded version of the Ender 3 printer manufactured by Creality, was employed for the printing of coatings (Fig. 1). This modified version incorporated a direct-drive extrusion system, enhancing its printing capabilities. In addition, an automatic bed leveling system, utilizing Bl-touch technology, was integrated into the Ender 3 3D printer, ensuring precise and consistent printing bed alignment. The extrusion and plate bed temperatures for the 3D printed filaments are detailed in Table 2. A 0.4 mm extrusion nozzle brass width was utilized.

Table 1. Technical Specifications of Graphene-Impregnated Polylactic Acid Raw Material

Specifications	*Typical value*
Tensile strength[a]	41 MPa
Tensile modulus[a]	2.6 GPa
Elongation at break[a]	4.7%
Flexural modulus[a]	2.8 GPa
Impact energy[a]	34 kJ/m^2
Specific gravity[a]	1.11 g/cm^3
Melt flow index (210°C/2.16 kg)	11.7 g/10 min
Diameter (tolerance)	1.75 ± 0.01 mm
Glass transition temperature	75°C
Melting temperature	160°C

[a]All the tests were done at the temperature 23°C.

The coating was printed with the external size and geometry of the control magnet. A cubic (10 × 10 × 10 mm) standard magnet, N35 NdFeB, with an original nickel coating, was used as the control. The coatings were printed with a 100% infill factor and zigzag fill patterns. The outer layer

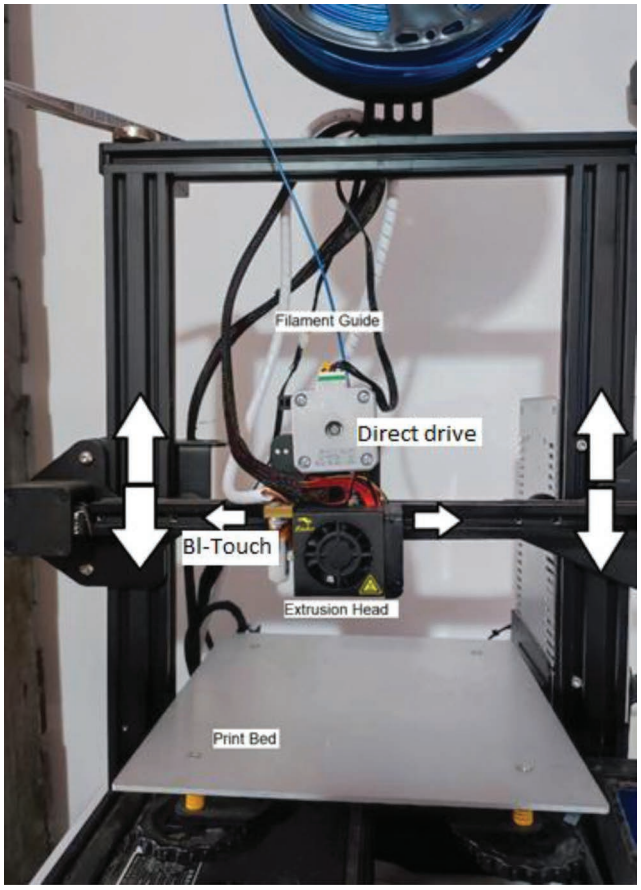

FIG. 1. Customized Ender 3 3D printer utilized to 3D print the coatings. Various components of the printer are shown, including the filament guide, direct drive extrusion head, print bed, and the (white arrows) of motion of the stepper motors.

Table 2. Extrusion and Plate Temperature of 3D Printed Coating

PLA filament	*Extrusion temperature, °C*	*Plate bed temperature, °C*
G-PLA	215	65

G-PLA, graphene-impregnated polylactic acid.

(shell) thickness of all printed coatings was two layers. The layer height was initialed by 0.05 mm on top and 0.05 mm on the bottom, forming a minimal coating width of 0.1 mm. The coating width (g) was increased by 0.1 mm (0.05 mm on top and 0.05 mm on bottom) in every printed coating. Typically, printed coatings and their internal fill characteristics are shown in Figure 2.

Immersion tests

The specimens were immersed in NaCl solutions with two concentrations, 0.5 and 1 M, for 30 days. This concentration is representative of the salinity found in coastal or marine areas where corrosion is a concern. The magnetized specimens were observed after different immersion times, specifically, 5, 15, and 30 days, to monitor the corrosion evolution with time. After weight loss test was conducted, the coupons were cleaned and dried. The weight of the coupons was then taken using electronic weighing scale. Full magnetization in a 6-T pulsed field was applied using a capacitive discharger, considering that this condition affects the corrosion behavior of magnets and other materials.[35–41]

Magnetic property measurements

Magnetic measurements of the magnetized samples were performed at room temperature using a closed magnetic circuit permeameter (hysteresis graph) after saturation in a pulsed magnetic field of 6 T. To achieve full magnetization, a very high magnetic field of at least three to five times the intrinsic coercivity was necessary.[42,43] The end faces of the test magnetized sample should be in intimate contact with the pole faces because there are always unavoidable small air gaps due to the surface roughness, poor parallelism of the sample or pole faces, or intentional shimming to protect delicate specimens from deformation or crushing.[43]

Using a coating to protect the magnet increases the gap and decreases the remanence; hence, the protective layer must be kept as thin as possible (if the magnet is to be used in very aggressive environments, such as wind generators[44] on or offshore, some flux losses would be tolerable to extend the life span of the turbine, and a good compromise between these two parameters is essential for reducing production costs). Since the axial-flux cubic magnet was employed, the significance of maintaining the G-PLA layer as thin as possible on the polar faces of the magnet becomes apparent. Conversely, there is no concern regarding the coating thickness on the lateral faces (shell) due to the lack of interaction with the magnetic flux in the closed circuit. Figure 3 illustrates a schematic representation of the axial-flux cubic magnet.

Results and Discussion

Figure 4 shows images of NdFeB N35 after immersion in 0.5 M NaCl solution at different times. Figure 4A–D corresponds to the immersion times of 5, 10, 15, and 30 days, respectively. After 5 days of immersion (Fig. 4A), pitting corrosion occurred, and small holes and dark spots appeared on the NdFeB N35 surface. After 10 days of immersion (Fig. 5B), corrosion began at the edges because the edges possessed higher energies. After 15 days of exposure (Fig. 4C), some wells were covered by irregular corrosion products, which blocked the diffusion channels, slowing the propagation of pitting corrosion. Finally, after 30 days of testing, the volume of the corrosion products increased and dispersed, and the corrosion intensified.

Figure 5 shows the photographs of NdFeB N35 after immersion in a 1 M NaCl solution at different times. Figure 5A–D corresponds to the immersion times of 5, 10, 15, and 30 days, respectively. The corrosion progress was similar to that observed in the 0.5 M NaCl test solution, although the corrosion propagation rate increased relative to that in the 0.5 M solution.

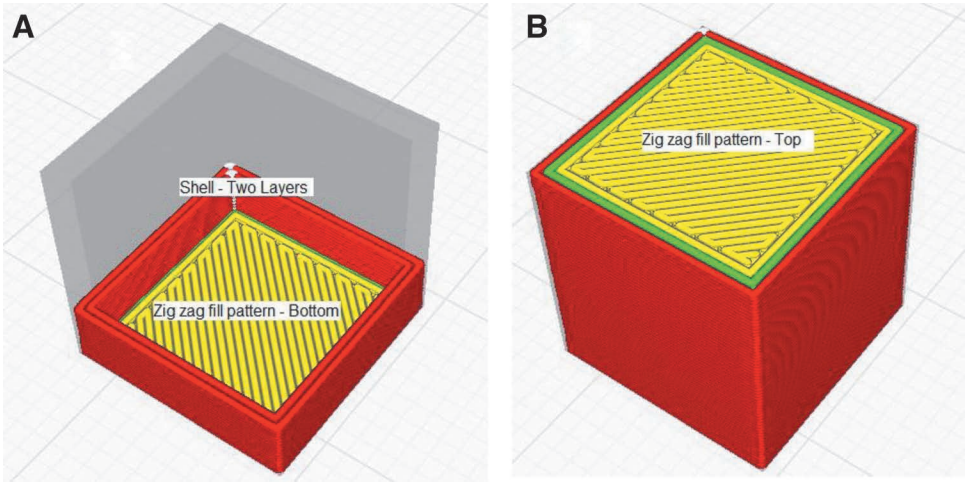

FIG. 2. Sections of coating modeled on Ultimaker Cura. **(A)** Zig-zag filling pattern of bottom coating and a two-layer shell, **(B)** completed coating.

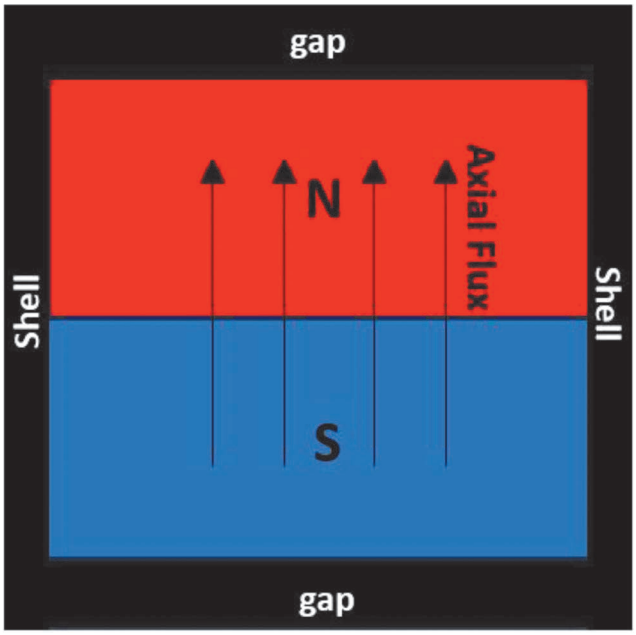

FIG. 3. Schematic representation of axial magnetic flux, gap, and shell in cubic NdFeB.

The poor corrosion resistance of these magnets is due to their high content of Nd and the coexistence of several phases in the microstructure, which are necessary to ensure the required magnetic properties The microstructure comprises of the ferromagnetic matrix-phase or Φ-phase ($Nd_2Fe_{14}B$) surrounded by intergranular ($Nd_{1+\epsilon}Fe_4B_4$) and Nd-rich (Nd_4Fe) phases regions consisting of B rich. According to Zhang et al.,[45] the corrosion susceptibility of NdFeB magnets is because of the lower potential of the Nd-rich phase compared to that of the matrix phase in NdFeB magnets. Consequently, Nd-rich phases preferentially undergo electrochemical reactions that release heat. The corrosion mechanisms in these magnets show regularity, with pitting corrosion occurring first, followed by intergranular corrosion, matrix phase detachment or dissolution from the NdFeB surface, and, finally, exposure of a new surface to the solution.

Figure 6 shows the photographs of NdFeB N35 magnets covered with a graphene-based coating created by 3D printing after immersion in a 1 M NaCl solution at different times. Figure 6A–D corresponds to the immersion times of 5, 10, 15, and 30 days, respectively. After 30 days of immersion (Fig. 6D), no corrosion product was observed in the 1 M NaCl solution. The thickness of the coating shown in Figure 6 is the minimum possible for the FDM 3D printing technology, which corresponds to 0.05 mm on the face of the cubic magnet.

The corrosion resistance of an NdFeB magnet can be analyzed by weight loss. After the immersion of the two NdFeB magnet samples with the standard nickel coating in NaCl solutions, their weight loss increased with increasing immersion time (Fig. 7) and NaCl concentration. This represents a percentage of weight loss of 8.5% and 14.3% for 0.5 M NaCl and 1 M NaCl solution, respectively. However, no weight loss occurred when the magnet was coated using a 3D printing process to obtain a layer with a thermoplastic polymer–graphene composite material.

Figure 8 shows the remanence as a function of the coating thickness. The remanence decreased from 1.17 T for the standard nickel-coated magnet, to 1.01 T, for the 0.5-mm-

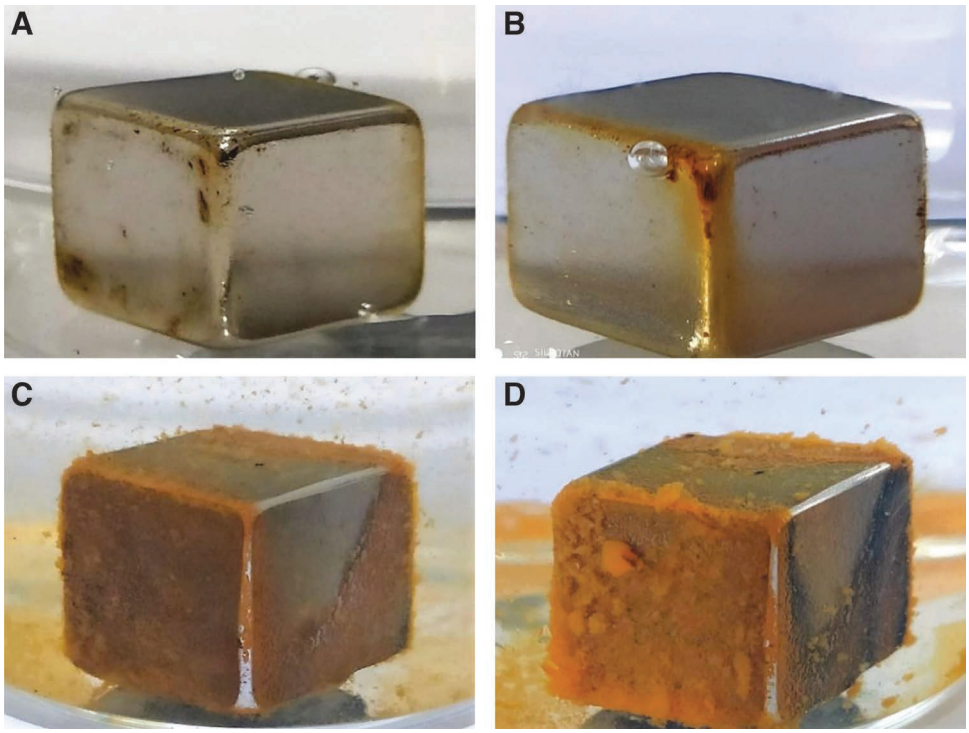

FIG. 4. Photo images of N35 NdFeB magnet immersed in 0.5 M NaCl solution for **(A)** 5 days, **(B)** 10 days, **(C)** 15 days, and **(D)** 30 days.

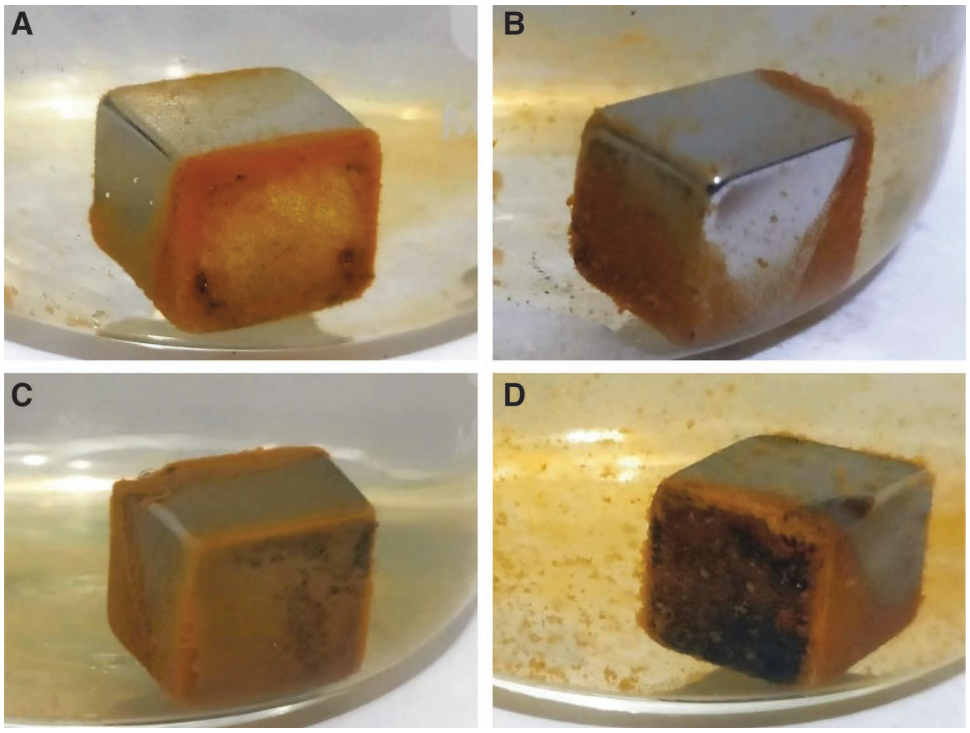

FIG. 5. Photo images of N35 NdFeB magnet immersed in 1 M NaCl solution for **(A)** 5 days, **(B)** 10 days, **(C)** 15 days, and **(D)** 30 days.

thick coating, which corresponded to a 13.3% loss of the total remanence. This was because of the increasing gap at which the magnetic field was measured. The loss in remanence due to the coating can be compensated for by using permanent magnet grades with higher remanence compared with N35 and is suitable for each required application, as shown in Table 3.[46] For instance, it is possible to increase the remanence by 26.5% using an N52 magnet instead of an N35 magnet, knowing that the gap produced by the coating will impact the final remanence of the project.

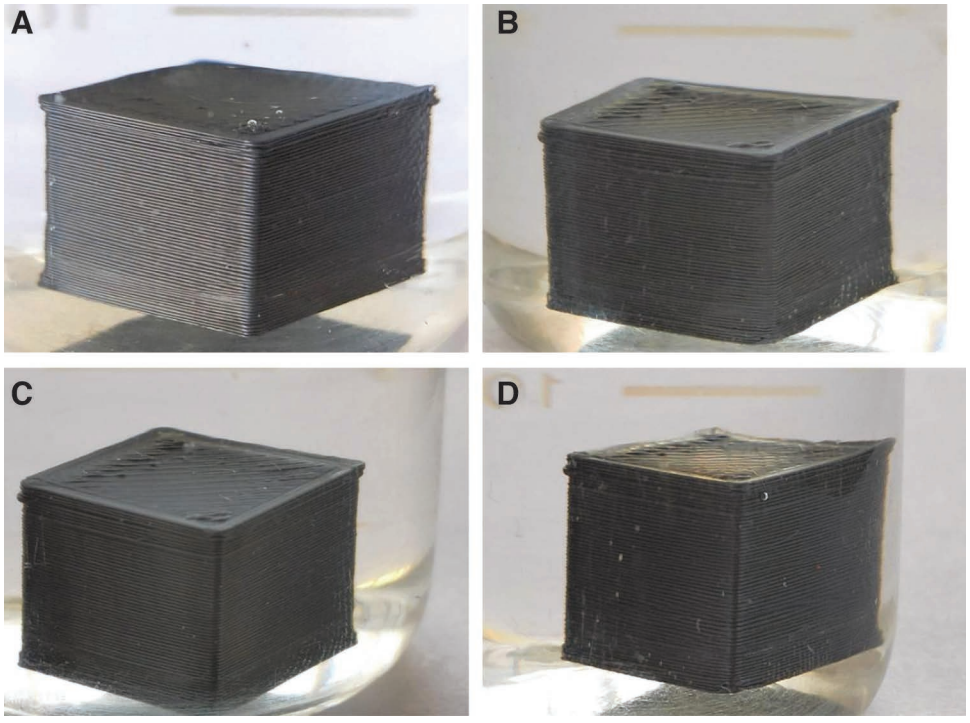

FIG. 6. Photo images of N35 NdFeB magnets covered with graphene-based coating by the 3D printing process. The magnets were immersed in 1 M NaCl solution for **(A)** 5 days, **(B)** 10 days, **(C)** 15 days, and **(D)** 30 days.

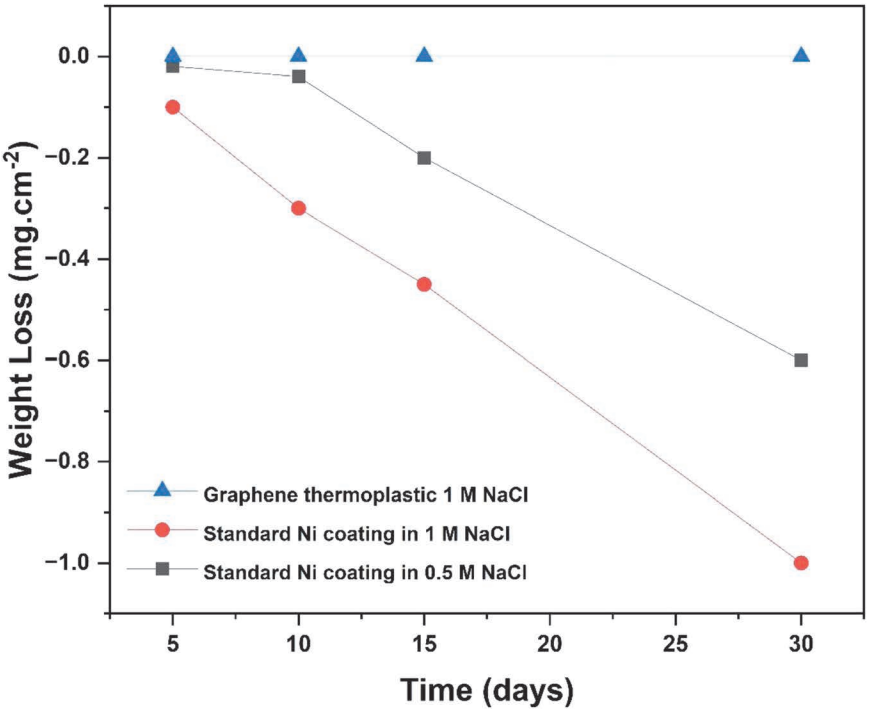

FIG. 7. Weight loss curves of NdFeB magnets immersed in NaCl solutions.

A long-term immersion test (6 months) in a 1 M NaCl solution showed that the G-PLA coating maintained the corrosion protection of the magnet. Given that PLA is a widely used biodegradable polymer in 3D printing prototyping, the biodegradation of G-PLA was not observed for the 1 M NaCl solution after 6 months of immersion. However, the magnet with only a nickel coating (standard) was significantly corroded before 6 months, showing that the standard nickel coating is insufficient to protect against corrosion in applications with direct exposure to NaCl environments.

A growing interest is emerging in the development of high-performance composites suitable for 3D printing, achieved through the introduction of nanomaterials with unique

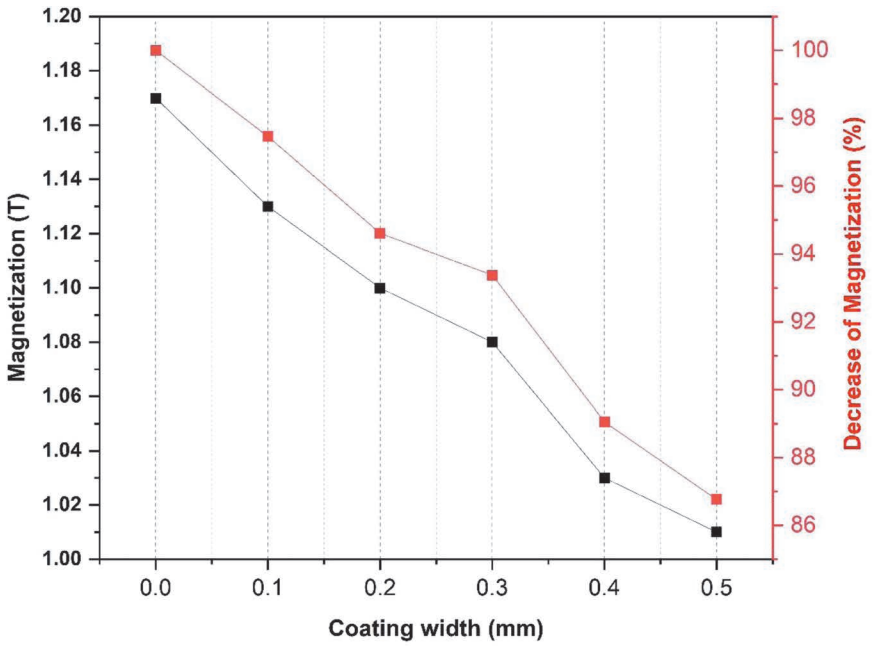

FIG. 8. Comparison between the magnetization (*black*) and the percentage of decrease in the magnetization (*red*) as a function of the increase of the G-PLA coating layer. G-PLA, graphene-impregnated polylactic acid.

Table 3. Magnetic Properties of Commercial-Grade Sintered Magnets Measured At Room Temperature (Maximum Operating Temperature 80°C)[45]

Grade[a]	*Remanence B_r, T*	*Inductive coercivity H_{cb}, kA/m*	*Intrinsic coercivity H_{cj}, kA/m*	*Energy product, kJ/m^3*
N35	1.170–1.220	868	955	263–287
N38	1.220–1.250	899	955	287–310
N40	1.250–1.280	907	955	302–326
N42	1.280–1.320	915	955	318–342
N45	1.320–1.380	923	955	342–366
N48	1.380–1.420	923	955	366–390
N50	1.400–1.450	796	876	382–406
N52	1.430–1.480	796	876	398–422

[a]The ''N'' designation is employed to categorize NdFeB magnets, with the addition of the magnet's maximum energy product, (BH)max.

properties, such as nanotubes, graphene, and their derivatives, into the polymeric matrix. The addition of graphene to polymer matrices has resulted in composites that exhibit superior mechanical strength, while maintaining their flexibility, as well as adaptable thermal and electrical conductivity owing to the graphene network in the matrix. Research has demonstrated particularly promising improvements in graphene-based thermal conductivities. With regard to the final application of electrical generators in wind turbines, which are largely exposed to the action of rain, wind, and severe temperature conditions, the use of PLA-graphene can result in greater resistance compared to PLA-only materials.[28]

The potential scalability of the 3D printing process for industrial applications is a crucial aspect to consider. The process can be enhanced in terms of adaptability and versatility, particularly in the production of complex geometries. It is important to emphasize that a basic model 3D printer was used for this study. Recognizing that professional-grade 3D printers can achieve thinner and more precise layers is essential, potentially mitigating the remanence loss effect. However, it is also pertinent to acknowledge that the described process comes with limitations. These limitations encompass constraints in material selection and manufacturing speed, which may impact the efficiency of the coating production.

Current coatings on NdFeB magnets are manufactured using the electroplating technique, which necessitates an initial pretreatment involving immersion in chemical agents to perform an initial etching, followed by the electroplating of nickel layers through chemical baths. The resulting coating possesses a flat surface, susceptible to removal through grinding or chemical processes. In contrast, the PLA coating presents a sustainable approach compared to traditional electroplating-based coatings. While chemical coatings often employ organic solvents and corrosive chemicals during application, the PLA coating is derived from a biodegradable polymer and employs a low-energy 3D printing process. This more sustainable approach not only mitigates adverse environmental impacts associated with chemical coatings but also enables material recycling and reusability, as the adhesion of PLA to the magnet's surface is superficial, facilitating facile removal.

Despite offering several advantages, the coating technique developed in this study suffers from a few limitations. First, any adhesive or coating between the magnets acts as an air gap, thus reducing the level of magnetism. Second, NdFeB magnets corrode extremely aggressively.

Depending on the application in which the magnets are used, it is worth reducing the remanence at the cost of protection. For example, a permanent-magnet synchronous generator is an alternative type of wind-turbine generator that is usually installed in coastal regions and offshores, represented by high levels of corrosion. This corrosion issue is aggravated by the environmental conditions of wind turbines. The corrosion of the Nd-rich phase located at the grain boundaries of NdFeB magnets results in the formation of neodymium hydroxide. The conversion of Nd to $Nd(OH)_3$ results in a large volume increase along the grain boundaries, leading to magnet degradation. This is affected by the geometry and grain structure of the magnet.[47,48]

Conclusion

In this study, we used a low-cost 3D printer to produce a new type of coating made of thermoplastic graphene on NdFeB commercial magnets. The coating increased the dimension for each face of the cubic sintered NdFeB magnet by 0.05 mm. The minimum coating thickness studied was 0.1 mm (0.05 mm at the top and 0.05 mm at the bottom), which was effective in protecting against corrosion in the 1 M NaCl solution. Under these conditions, the remanence loss was the lowest. The increase in corrosion protection in comparison with that provided by nickel coating, which is usually used in commercial magnets, was significant. Magnetic loss can be overcome by employing permanent magnets of commercial grade with higher remanence.

Acknowledgments

The authors wish to thank the Federal Institute of Education, Science, and Technology of the São Paulo Campus São José dos Campos (IFSP-SJC), and the Nuclear and Energy Research Institute (IPEN) of the University of São Paulo (USP) for their financial support. The authors also wish to thank the National Council for Scientific and Technological Development of Brazil for financial support (MCTIC/CNPq No. 28/2018–Universal 431667/2018-7).

Authors' Contributions

J.C.S.C., designed, planned the experimental procedure, sample manufacturing, and characterization procedures, and conceived the original idea of this article, as well the original draft version.

I.C., as corrosion material expert, contributed on the theoretical and experimental corrosion tests, and discussion and review of the present article.

R.N.d.F., as Magnetism and Magnetic Materials expert, contributed to the supervision, theoretical discussion, and review of the present article.

All the authors provided critical feedback and helped to improve this research.

Author Disclosure Statement

No competing financial interests exist.

Funding Information

Rubens Nunes de Faria Jr. is also grateful for the support received from project INCT-PATRIA (Contract No. FAPESP 14/50887-4, CAPES 23038.000776/2017-54, and CNPq 465719/2014-7).

References

1. Bilgili M, Yasar A, Simsek E. Offshore wind power development in Europe and its comparison with onshore counterpart. Renew Sustain Energy Rev 2011;15(2):905–915; doi: 10.1016/j.rser.2010.11.006
2. El-Moneim A, Gebert A. Electrochemical characterization of galvanically coupled single phases and nanocrystalline NdFeB-based magnets in NaCl solutions. J Appl Electrochem 2003;33:795–805; doi: 10.1023/A:1025548411091
3. Zhang P, Ma T, Liang L, et al. Improvement of corrosion resistance of Cu and Nb co-added NdFeB sintered magnets. Mater Chem Phys 2014;147(3):982–986; doi: 10.1016/j.matchemphys.2014.06.046
4. Yu L, Wen Y, Yan Y. Effects of Dy and Nb on the magnetic properties and corrosion resistance of sintered NdFeB. J Magn Magn Mater 2004;283(2–3):353–356; doi: 10.1016/j.jmmm.2004.06.006
5. Yang X, Li Q, Zhang S, et al. Electrochemical corrosion behaviors and protective properties of Ni–Co–TiO_2 composite coating prepared on sintered NdFeB magnet. Mater Corros 2010;61(7):618–625; doi: 10.1002/maco.200905449
6. Huang Y, Li H, Zuo M, et al. Corrosion resistance of sintered NdFeB coated with SiC/Al bilayer thin films by magnetron sputtering. J Magn Magn Mater 2016;409:39–40; doi: 10.1016/j.jmmm.2016.02.006
7. Chen E, Peng K, Yang W, et al. Effects of Al coating on corrosion resistance of sintered NdFeB magnet. Trans Nonferrous Met Soc China 2014;24(9):2864–2869; doi: 10.1016/S1003-6326(14)63419-1
8. Zhang K, Wang Z, He J, et al. Coupling effects of hydrogen and Dy/Nb on magnetic properties of sintered NdFeB magnets. Int J Hydrogen Energy 2022;47(30):14027–14038; doi: 10.1016/j.ijhydene.2022.02.154
9. Mao S, Yang H, Song Z, et al. Corrosion behaviour of sintered NdFeB deposited with an aluminum coating. Corros Sci 2011;53(5):1887–1894; doi: 10.1016/j.corsci.2011.02.006
10. Rada M, Gebert A, Mazilu I, et al. Corrosion studies on highly textured Nd–Fe–B sintered magnets. J Alloys Compd 2006;415(1–2):111–120; doi: 10.1016/j.jallcom.2005.07.063
11. Kim T, Lee S, Kim H, et al. Simultaneous application of Dy–X (X = F or H) powder doping and dip-coating processes to Nd–Fe–B sintered magnets. Acta Mater 2015;93:95–104; doi: 10.1016/j.actamat.2015.04.019
12. Isotahdon E. Corrosion Losses, Mechanisms and Protection Strategies for Sintered Nd-Fe-B Magnets. The Tampere University of Technology. Publication: Finland; 2017.
13. Drak M, Dobrzański LA. Corrosion of Nd-Fe-B permanent magnets. J Achiev Mater Manuf Eng 2007;20(1–2):239–242.
14. Kappel W, Codescu MM, Stancu N, et al. Evaluation of the corrosion behavior for the permanent magnets based on rare earth, used in aeronautical industry. J Optoelectronics Adv Mater 2006;8(2):523–525.
15. Zhou Q, Liua ZW, Zhong XC, et al. Properties improvement and structural optimization of sintered NdFeB magnets by non-rare earth compound grain boundary diffusion. Mater Des 2015;86:114–120; doi: 10.1016/j.matdes.2015.07.067
16. Wang H, Li A, Li W. Effect of Pr and Dy substitution on the impact resistance of sintered NdFeB magnets. Intermetallics 2006;15(7):985–988; doi: 10.1016/j.intermet.2006.11.001
17. Schultz L, El-Aziz AM, Barkleit G, et al. Corrosion behavior of Nd–Fe–B permanent magnetic alloys. Mater Sci Eng A 1999;267(2):307–313; doi: 10.1016/S0921-5093(99)00107-0
18. Raza MA, Rehman ZU, Ghauri FA, et al. Corrosion study of electrophoretically deposited graphene oxide coatings on copper metal. Thin Solid Films 2016;620:150–159; doi: 10.1016/j.tsf.2016.09.036
19. Oliveira MCL, Antunes RA. Graphene-based coatings for magnesium alloys: Exploring the correlation between coating architecture, deposition methods, corrosion resistance and materials selection. Corros Rev 2022;40(5):427–451; doi: 10.1515/corrrev-2022-0004
20. Kiran NU, Dey S, Singh BP, et al. Graphene coating on copper by electrophoretic deposition for corrosion prevention. Coatings 2017;7(12):214; doi: 10.3390/coatings7120214
21. He W, Zhu L, Chen H, et al. Electrophoretic deposition of graphene oxide as a corrosion inhibitor for sintered NdFeB, Appl Surf Sci 2013;279:416–423; doi: 10.1016/j.apsusc.2013.04.130
22. Tong Y, Bohm S, Song M. Graphene based materials and their composites as coatings. Austin J Nanomed Nanotechnol 2014;1(1):1003.
23. Raza MA, Ahmad A, Ghauri FA, et al. Graphene oxide coating for improved corrosion resistance of NdFeB. NUST J Eng Sci 2017;10(1):14–18; doi: 10.24949/njes.v10i1.200
24. Mondal J, Marandi M, Kozlova J, et al. Protection and functionalizing of stainless steel surface by graphene oxide-polypyrrole composite coating. J Chem Chem Eng 2014;8:786–793.
25. Xie Y, Chen M, Xie D, et al. A fast, low temperature zinc phosphate coating on steel accelerated by graphene oxide. Corros Sci 2017;128:1–8; doi: 10.1016/j.corsci.2017.08.033
26. Guo N, Leu MC. Additive manufacturing: Technology, applications, and research needs. Front Mech Eng 2013;8:1–29; doi: 10.1007/s11465-013-0248-8
27. Ngo TD, Kashani A, Imbalzano G, et al. Additive manufacturing (3D printing): A review of materials, methods, applications and challenges. Compos B Eng 2018;143:172–196; doi: 10.1016/j.compositesb.2018.02.012
28. Bustillos J, Montero D, Nautiyal P, et al. Integration of graphene in poly (lactic) acid by 3D printing to develop

creep and wear-resistant hierarchical nanocomposites. Polym Compos 2018;39(11):3877–3888; doi: 10.1002/pc.24422
29. Rarani MH, Afarani MR, Zahedi AM. Mechanical characterization of FDM 3D printing of continuous carbon fiber reinforced PLA composites. Compos B Eng 2019;175:107147; doi: 10.1016/j.compositesb.2019.107147
30. Caminero MA, Chacón JM, Plaza EG, et al. Additive manufacturing of PLA-based composites using fused filament fabrication: Effect of graphene nanoplatelet reinforcement on mechanical properties, dimensional accuracy and texture. Polymers 2019;11(5):799; doi: doi.org/10.3390/polym11050799
31. Mittal G, Dhand V, Rhee KY, et al. A review on carbon nanotubes and graphene as fillers in reinforced polymer nanocomposies. J Ind Eng Chem 2015;21:11–25; doi: 10.1016/j.jiec.2014.03.022
32. Vidakis N, Petousis M, Savvakis K, et al. A comprehensive investigation of the mechanical behavior and the dielectrics of pure polylactic acid (PLA) and PLA with graphene (GnP) in fused deposition modeling (FDM). Int J Plast Technol 2019;23:195–206.; doi: 10.1007/s12588-019-09248-1
33. Camargo JC, Machado AR, Almeida EC, et al. Mechanical properties of PLA-graphene filament for FDM 3D printing. Int J Adv Manuf Technol 2019;103:2423–2443; doi: 10.1007/s00170-019-03532-5
34. Haydale. Available from: https://www.haydale.com/products/ [Last accessed: August 20, 2023].
35. Moore M, Sueptitz R, Gebert A, et al. Impact of magnetization state on the corrosion of sintered Nd–Fe–B magnets for e-motor applications. Mater Corros 2014;65(9):891–896; doi: 10.1002/maco.201206978
36. Ang LY, Othman NK, Jalar A, et al. The effect of magnetic field on copper in various corrosive medium. AIP Conf Proc 2014;1614(1):26–29; doi: 10.1063/1.4895164
37. Parapurath S, Ravikumar A, Vahdati N, et al. Effect of magnetic field on the corrosion of API-5L-X65 steel using electrochemical methods in a flow loop. Appl Sci 2021;11(19):9329; doi: 10.3390/app11199329
38. Mitre CIN, Tosin G, Colnago LA. In-operando analysis of the corrosion patterns and rates under magnetic fields using metallic film. NPJ Mater Degrad 2022;6:24; doi: 10.1038/s41529-022-00233-5
39. Zhang Y, Wang Y, Zhao S, et al. Effect of magnetic field on the corrosion behaviour of carbon steel in static seawater. Int J Electrochem Sci 2019;14:11279–11288; doi: 10.20964/2019.12.14
40. Nasher LSH, Shalash LABT; Study the effect of magnetic field on the corrosion of steel in sodium chloride solution (NaCl). Misan J Acad Stud 2010;9(17):30–38
41. Costa I, Oliveira MCL, Melo HG, Faria RN; The effect of the magnetic field on the corrosion behavior of Nd–Fe–B permanent magnets. J Magn Magn Mater 2004;278(3):348–358; doi: 10.1016/j.jmmm.2003.12.1320
42. Bavendiek G, Müller F, Steentjes S, et al. Modeling of history-dependent magnetization in the finite element method on the example of a postassembly rotor magnetizer. Int J Numer Model 2020;33:e2674; doi: 10.1002/jnm.2674
43. Standard Test Method for Magnetic Properties of High-Coercivity Permanent Magnet Materials Using Hysteresigraphs.
44. Isotahdon E, Huttunen-Saarivirta E, Kuokkala VT; Development of magnetic losses during accelerated corrosion tests for Nd-Fe-B magnets used in permanent magnet generators. Corrosion 2016;72(6):732–741; doi: 10.5006/2037
45. Zhang K, Fan E, He J, et al. Long-term effects of electrochemical corrosion on magnetic properties of sintered NdFeB magnets. J Magn Magn Mater 2021;538:168309; doi: 10.1016/j.jmmm.2021.168309
46. Magnet Expert. Magnetic properties of neodymium magnets; 2023. Available from: https://www.magnetexpert.com/magnetic-properties-of-neodymium-magnets-i694 [Last accessed: June 14, 2023].
47. Isotahdon E, Huttunen-Saarivirta E, Kuokkala VT, et al. Corrosion losses in sintered (Nd, Dy)–Fe–B magnets for different geometries. IEEE Magnet Lett 2016;7:1–4; doi: 10.1109/LMAG.2015.2501404
48. Ni J, Ma T, Yan M; Improvement of corrosion resistance in Nd–Fe–B magnets through grain boundaries restructuring. Mater Lett 2012;75:1–3; doi: 10.1016/j.matlet.2012.01.100

Address correspondence to:
Julio Cesar Serafim Casini
Federal Institute of Education, Science and Technology of São Paulo Campus
São José dos Campos–IFSP-SJC
Rod. Pres. Dutra, km 145
s/n Jardim Diamante
São José dos Campos, SP 12223-201
Brazil

E-mail: julio.casini@ifsp.edu.br